A 3-Player Game with Bounded Rationality Concerning Ecology Compensation and Environmental Tax Policies

Xiaozhu Chen (chenxiaozhu529@nuaa.edu.cn)
Nanjing University of Aeronautics and Astronautics https://orcid.org/0000-0002-4200-059X
Jixiang Zhang
Nanjing University of Aeronautics and Astronautics

Research Article

Keywords: Nitrogen cascade, 3-player game, Ecology compensation, Nash equilibrium, Chaos

Posted Date: April 19th, 2022

DOI: https://doi.org/10.21203/rs.3.rs-1544715/v1

A 3-Player Game with Bounded Rationality Concerning Ecology Compensation and Environmental Tax Policies

Jixiang Zhang[1]* Xiaozhu Chen[1]*

1.College of Economics and Management, Nanjing University of Aeronautics and Astronautics, Nanjing, 211106, China.
Correspondence should be addressed to Xiaozhu Chen; chenxiaozhu529@nuaa.edu.cn

Abstract: In the face of environmental hazards caused by low nitrogen utilization efficiency, this paper constructed a 3-player game model which contains local governments, peasant households, and polluting enterprises with bounded rationality, all of which take part in the nitrogen cascade in the watersheds. The Nash equilibrium points and local stability of the dynamical systems were investigated. Complex dynamics i.e. bifurcation and chaos arise from the variation of some parameters of the model, including the adjustment speed of decision-making of a boundedly rational player. Numerical simulations were rendered to manifest bifurcation, chaos, maximal Lyapunov exponent, strange attractor, and sensitive dependence on initial conditions. Chaos control of the dynamic systems was discussed using the delayed feedback scheme. Research results indicate that whereas the adjustment speed of players has a destabilizing effect, a proper increment of the ecological compensation or environmental tax rate will restore the local stability of the system. Moreover, while the excessive adjustment speed has caused the system to behave chaotically, an increase of the feedback controller can eliminate chaos and achieve a stable market.

Key words: Nitrogen cascade; 3-player game; Ecology compensation; Nash equilibrium; Chaos

1. Introduction

Despite its relevance to multiple UN Sustainable Development Goals (SDGs) [1], nitrogen (N) pollution still lacks broad visibility and coordinated global governance. A new goal to ‘‘halve nitrogen waste’’ by 2030 would save US$100 billion annually, contributing to post-coronavirus economic recovery [2]. The eighth International Nitrogen Initiative Conference (INI), held in 2021, emphasized that N fertilizer application and livestock breeding are still the largest sources of reactive N emissions. Furthermore, increasingly industrial and agricultural activities by humans have caused numerous hazards to the ecological environment and biodiversity [3]. For the time being, it was estimated that two-thirds of the coastal rivers and bays in the US are degraded from the growing crisis of nutrient pollution [4]. In an endeavor to enhance N utilization efficiency, local governments in the watersheds are formulating ecological compensation and environmental tax policies to encourage green production. Therefore, it is vital to investigate the game of interests of the main decision-makers in the N cascade, namely the local governments, peasant households, and polluting enterprises.

Recent research on N utilization efficiency has mainly focused on threefold [5]. Firstly, the Nutrient Analysis Method was adopted for screening genotypes of crops to enhance N utilization efficiency. S. Das et al. [6] studied the linear relationship between rice yield and three physiological indexes, and recommended the evaluation of N

* These authors contributed to the work eqully and should be regarded as co-first authors.

efficiency performance at lower N levels. Secondly, when the watersheds were taken as the boundaries, the N footprint analysis was carried out based on the N-calculator model. Dukes et al. [7] estimated the dynamic change of N footprint in Baltimore, and analyzed the relationship between water quality response and N utilization efficiency. Leach et al. [8] analyzed the effects of various levels of N application on the N input and output changes in farmlands and concluded that the reducing N fertilizer effectively improved the crop yield and N utilization efficiency. Thirdly, the environmental load caused by N flow is studied based on the material flow method (MFA) [9]. The N flux and flow efficiency in the United States were investigated based on NFA [10], indicating that scientific fertilization and ecological breeding could effectively reduce the environmental N load.

Currently, based on Game Theory, literature has demonstrated the impacts of environmental policies on interest-related decision-makers in the watersheds. To begin with, a game model of ecological compensation between upstream and downstream governments was established to study the evolutionary stability strategies (ESS). An evolutionary game between upstream and downstream governments under watershed ecological compensations was determined [11]. It was found that the policy-making of ecological compensations necessitates the applicable intervention of central governments. Shen et al. [12] studied the evolutionary game scenario of ecological subsidy policies made by upstream and downstream governments of the Taihu Lake Basin, and put forward the conditions for reaching ESS under different circumstances. In addition, an evolutionary game between local governments and industrial enterprises is analyzed based on ecological compensation and environmental tax systems. Barcena-Ruiz [13] studied the impacts of key factors such as the government's pollution tax rate and the enterprise's pollutant treatment technology level on the game system. Jorgensen [14] constructed an ecological compensation model for upstream and downstream governments and polluting enterprises, and proposed that both compensation and punishment mechanisms should be established for emission reduction in river basins. To summarize, we can infer that relevant research on ecological policies in the watersheds is mainly between governments and industrial enterprises using the Evolutionary Game Model. Whereas it is essential to take peasant households into account to attain the specific goal of enhancing nitrogen cascade utilization efficiency.

Given that mutual and concerted efforts of decision-makers are indispensable in formulating and implementing ecological policies, this paper constructs a 3-player game model based on the Optimal Dynamic Response theory to digest the dynamic behaviors of boundedly rational players. The Optimal Response Dynamics mechanism is originally designed to analyze and discuss small groups with high rationality and quick learning ability. Bischi et al. [15] modelled a dynamic Cournot duopoly game and analyzed the players' local adjustment strategy according to the marginal profit in the last period. Numerous scholars have further explored the dynamical phenomena of the system i.e. bifurcation and chaos. Puu [16] first analyzed the complex dynamical phenomena including strange attractors with fractal dimensions based on a Cournot duopoly model. Agiza et al. [17] studied a Cournot duopoly and triopoly game with adaptive expectations through numerical simulations of chaos and bifurcation. Various methods have been applied to chaos control. Elsadany et al. [18] established a Cournot triopoly game model based on the nonlinear cost function and concluded that delayed decision can expand the Nash equilibrium stability region effectively. Paula [19] classified chaos control methods as OGY methods, multiparameter methods, and time-delayed feedback methods, and presented a comparative analysis of the capability of each method.

This study aims to investigate the dynamic behaviors of a 3-player game involving local governments, peasant households, and polluting enterprises with bounded rationality, all of which participate in the N cascade in the watersheds. In an attempt to improve N utilization efficiency, local governments ought to establish reasonable ecological compensation and environmental tax policies. Under the influence of the policy implementation intensity, peasant households and polluting enterprises will adjust their optimal decision-making standards of the mode of production. It is crucial to investigate the dynamic behaviors of boundedly rational players, as relevant suggestions

can be provided for improving nitrogen cascade utilization efficiency in practice.

The paper was organized as follows. In Section 2, a 3-player game involving governments, peasant households, and polluting enterprises with bounded rationality was modeled. In Section 3, the Nash equilibrium points and local stability of the dynamic systems were analyzed, and the existing condition and local stability range of the equilibria were given. In Section 4, numerical simulations to manifest complex dynamics i.e. bifurcation and chaos were rendered, and the impacts of adjustment speed, ecological compensation, and tax policies on the local stability of the system were then explored. In Section 5, the control of chaos based on the delayed feedback method was discussed. In Section 6, research conclusions were summarized and policy suggestions were proposed.

2. Model construction and parameter determination

In this chapter, a 3-player game model which contains local governments, peasant households, and polluting enterprises with bounded rationality was constructed. Assuming that the 3 players participating in the N cascade in the watersheds think with different strategies to make the optimal decision. To elaborate, the optimal decision-making standard of local governments is to formulate effective ecological compensation and environmental tax policies to ensure sustainable development, maximize total utility and improve social welfare. Whereas the optimal decision-making standard of peasant households is to decide the appropriate agricultural output and production mode in response to the ecological compensation policy to maximize their interests. From the perspective of the polluting enterprises, the optimal decision-making purpose is to choose the appropriate mode of operation and treatment intensity of nitrogenous pollutants to maximize their total utility. The definitions of the main variables and parameters in the model are shown in Table 1.

Table 1: Definitions of main parameters

Notation	Definition
$x(t)$	Local governments' policy implementation intensity at period t
$y(t)$	Peasant households' agricultural output at period t
$z(t)$	Polluting enterprises' treatment intensity of nitrogenous pollutants at period t
σ	Supervisory cost under ideal conditions
β	Ecological compensation per unit agricultural output
p	Price of agricultural products
a	Highest market price of agricultural products
b	Agricultural product price sensitivity coefficient
ω	Impact coefficient of policy implementation on green production
k	Level of realization of green production
c_1	Unit technical cost for green production
φ	Unit additional revenue from green production
s	Coefficient of social welfare caused by green production
t_1	Value-added tax rate of agricultural products
t_2	Income tax rate for polluting enterprises
t_3	Environmental tax rate for polluting enterprises
ρ	Ecological compensation for the treatment of unit nitrogenous pollutants
μ	Total industrial output of polluting enterprises
P	Total profit of polluting enterprises
e	Nitrogen emissions per unit output of polluting enterprises

θ	Impact coefficient of policy implementation on nitrogenous pollutants treatment
γ	Environment damage caused by unit nitrogen emission
c_2	Unit treatment cost of nitrogenous pollutants

The game model satisfies the following premises:

(1) For local governments, when the intensity of policy implementation reaches the ideal conditions, the supervisory cost is σ, hence the actual supervisory cost is σx. Local governments monitor the production mode of peasant households by testing indicators such as the amount of pesticide residues in the soil. Ecological compensations are given to peasants who meet the standard. The ecological compensation set for peasant households is β per unit agricultural output, and the value-added tax for agricultural products is t_1. The income tax rate set for polluting enterprises is t_2, the environmental tax rate is t_3, and the ecological compensation for the treatment of unit nitrogen pollutants is denoted as ρ.

(2) For peasant households, the agricultural product value-added tax under the production y can be described as $t_1 y$. The price p of an agricultural product is determined by the inverse demand function $p = a - by(a, b > 0)$. Green production is carried out through technologies such as reducing nitrogen fertilizer, using organic fertilizers, and cleaning livestock and poultry manure. The yield of green products can be described as $M = \omega x + ky$. The total technical cost to be paid is $c_1 M$, and the ecological compensation obtained is βMx. The realization of sustainable development brings additional benefits to peasant households as φM and improves social welfare as sM.

(3) For polluting enterprises, the profit income tax to be paid is $t_2 P$. Since the treatment of N-containing pollutants is affected by the intensity of policy implementation, the N reduction amount can be described as $R = \theta x + \mu z$. Accordingly, the total cost of the treatment of N-containing pollutants is $c_2 R$, and the ecological compensation given to polluting enterprises is $\rho R x$. The total N emissions can be expressed as a linear function of total industrial output, indicated as $e\mu$, therefore the final N emission is $e\mu - R$. The corresponding environmental tax to be paid is $t_3(e\mu - R)x$, and the ecological damage is estimated at $\gamma(e\mu - R)$.

Therefore, at period t, the utility function expressions of local government, peasant households, and polluting enterprises are as follows (Eq. 2.1):

$$\begin{cases} \Pi_1(t) = -\sigma x + t_1 y + (s - \beta x)(\omega x + ky) + t_2 P + (t_3 x - \gamma)[e\mu - (\theta x + \mu z)] - \rho x(\theta x + \mu z) \\ \Pi_2(t) = (a - by - t_1)y + (\omega x + ky)(\varphi - c_1 + \beta x) \\ \Pi_3(t) = (1 - t_2)P + (\rho x - c_2)(\theta x + \mu z) - [e\mu - (\theta x + \mu z)]t_3 x \end{cases} \tag{2.1}$$

Then, the marginal utilities of the 3 players are as follows (Eq. 2.2):

$$\begin{cases} \Phi_1 = \dfrac{\partial \Pi_1(t)}{\partial x(t)} = -\sigma + s\omega + \gamma\theta + t_3 e\mu - 2(\beta\omega + \theta t_3 + \rho\theta)x - \beta k y - (t_3 + \rho)\mu z \\ \Phi_2 = \dfrac{\partial \Pi_2(t)}{\partial y(t)} = k(\varphi - c_1 + \beta x) - 2by \\ \Phi_3 = \dfrac{\partial \Pi_3(t)}{\partial z(t)} = \mu[(\rho + t_3)x - c_2] \end{cases} \tag{2.2}$$

In actuality, restricted by technical conditions and incomplete information, game players with bounded rationality are incapable of accurately estimating the market demand in the next period. According to relevant research, their main basis of making optimal decisions is the local estimate of their marginal utility. The decision-making of local government, peasant households, and polluting enterprises has the following the nonlinear map $T(x(t), y(t), z(t)) \rightarrow (x(t+1), y(t+1), z(t+1))$, which is defined by Eq. 2.3

$$T:\begin{cases} x(t+1) = x(t) + \alpha_1 x(t)\Phi_1 \\ y(t+1) = y(t) + \alpha_2 y(t)\Phi_2 \\ z(t+1) = z(t) + \alpha_3 z(t)\Phi_3 \end{cases} \tag{2.3}$$

where $\alpha_i (i = 1,2,3)$ is a positive function that signifies the adjustment speed of each player in the light of his computed marginal profit. For ease of calculation, we denote $U = -\sigma + s\omega + \gamma\theta + t_3 e\mu$, $V = 2(\beta\omega + \theta t_3 + \rho\theta) > 0$, $W = t_3 + \rho > 0$. Thus, the dynamical system is described by Eq. 2.4

$$\begin{cases} x(t+1) = x(t)\left[1 + \alpha_1\left(U - Vx(t) - \beta k y(t) - W\mu z(t)\right)\right] \\ y(t+1) = y(t)\left\{1 + \alpha_2\left[k\left(\varphi - c_1 + \beta x(t)\right) - 2by(t)\right]\right\} \\ z(t+1) = z(t)[1 + \alpha_3\mu(Wx(t) - c_2)] \end{cases} \tag{2.4}$$

3. Nash Equilibrium Points and Local Stability

In this study, the dynamic behaviors of the game model were discussed through the Nash equilibria and the local stability of the system. We defined the equilibrium points of the dynamic game as nonnegative fixed points of the system (2.4), which were obtained by setting $x(t+1) = x(t)$, $y(t+1) = y(t)$, $z(t+1) = z(t)$. It was solved that the algebraic system (2.4) has six equilibria (Eq. 3.1):

$$\begin{cases} E_0 = (0,0,0) \\ E_1 = \left(\frac{U}{V}, 0, 0\right) \\ E_2 = \left(0, \frac{k(\varphi - c_1)}{2b}, 0\right) \\ E_3 = \left(\frac{c_2}{W}, 0, \frac{UW - Vc_2}{W^2\mu}\right) \\ E_4 = \left(\frac{2bU - \beta k^2(\varphi - c_1)}{2bV + \beta^2 k^2}, \frac{k\{(\varphi - c_1)(2bV + \beta^2 k^2) + \beta[2bU - \beta k^2(\varphi - c_1)]\}}{2b(2bV + \beta^2 k^2)}, 0\right) \\ E_* = (x^*, y^*, z^*) = \left(\frac{c_2}{W}, \frac{k[(\varphi - c_1)W + c_2\beta]}{2bW}, \frac{2bWU - 2bVc_2 - \beta k^2[(\varphi - c_1)W + c_2\beta]}{2bW^2\mu}\right) \end{cases} \tag{3.1}$$

where E_0, E_1, E_2, E_3 and E_4 represent the boundary equilibria, while the equilibrium E_5 is the unique Nash equilibrium when $(\varphi - c_1)W + c_2\beta > 0$, $2b(WU - Vc_2) - \beta k^2[(\varphi - c_1)W + c_2\beta] > 0$.

The analysis on the local stability of the equilibria depends on the eigenvalues of the Jacobian matrix J of the three-dimensional system (2.4) by the Eq. 3.2:

$$J = \begin{bmatrix} 1 + \alpha_1(U - 2Vx - \beta k y - W\mu z) & -x\alpha_1\beta k & -x\alpha_1 W\mu \\ \alpha_2 k\beta y & 1 + \alpha_2[k(\varphi - c_1 + \beta x) - 4by] & 0 \\ \alpha_3\mu W z & 0 & 1 + \alpha_3(Wx - c_2) \end{bmatrix} \tag{3.2}$$

Lemma 1. *The boundary equilibria E_0, E_1, E_2, E_3 and E_4 of the system (2.4) are saddle points (unstable equilibrium points).*

Proof. To prove this result, we estimate the eigenvalues of the Jacobian matrix J at each boundary equilibrium point. At E_0 the Jacobian matrix J takes the diagonal form:

$$J(E_0) = \begin{bmatrix} 1 + \alpha_1 U & 0 & 0 \\ 0 & 1 + \alpha_2 k(\varphi - c_1) & 0 \\ 0 & 0 & 1 - \alpha_3 c_2 \end{bmatrix} \tag{3.3}$$

whose eigenvalues are $\lambda_1 = 1 + \alpha_1 U$, $\lambda_2 = 1 + \alpha_2 k(\varphi - c_1)$, $\lambda_3 = 1 - \alpha_3 c_2$.It is evident on condition that $2b(WU - Vc_2) - \beta k^2[(\varphi - c_1)W + c_2\beta] > 0$, $U = -\sigma + s\omega + \gamma\theta + t_3\lambda\mu > 0$. Since α_1, U are positive constants then $\lambda_1 > 1$. Hence the equilibrium point E_0 is a saddle point.

At E_1 the Jacobian matrix J takes the upper triangular form as shown in Eq. 3.4:

$$J(E_1) = \begin{bmatrix} 1-\alpha_1 U & -\frac{\alpha_1 \beta k U}{V} & -\frac{\alpha_1 W \mu U}{V} \\ 0 & 1+\alpha_2 k\left(\varphi - c_1 + \frac{\beta U}{V}\right) & 0 \\ 0 & 0 & 1+\frac{\alpha_3 W U}{V} \end{bmatrix} \tag{3.4}$$

whose eigenvalues are $\lambda_1 = 1-\alpha_1 U$, $\lambda_2 = 1+\alpha_2 k\left(\varphi - c_1 + \frac{\beta U}{V}\right)$, $\lambda_3 = 1+\frac{\alpha_3 W U}{V}$. Since α_3, W, U, V are positive constants then $\lambda_2 > 1$. Hence the equilibrium point E_1 is a saddle point.

At E_2 the Jacobian matrix J takes the lower triangular form (Eq. 3.5):

$$J(E_2) = \begin{bmatrix} 1+\frac{[2bU-\beta k^2(\varphi - c_1)]\alpha_1}{2b} & 0 & 0 \\ \frac{\alpha_2 k^2 \beta(\varphi - c_1)}{2b} & 1-\alpha_2 k(\varphi - c_1) & 0 \\ 0 & 0 & 1-\alpha_3 c_2 \end{bmatrix} \tag{3.5}$$

whose eigenvalues are $\lambda_1 = 1+\frac{[2bU-\beta k^2(\varphi - c_1)]\alpha_1}{2b}$, $\lambda_2 = 1-\alpha_2 k(\varphi - c_1)$, $\lambda_3 = 1-\alpha_2 k(\varphi - c_1)$. It is evident on condition that $2b(WU - Vc_2) - \beta k^2[(\varphi - c_1)W + c_2\beta] > 0$, $2bU - \beta k^2(\varphi - c_1) > 0$. Since α_1, b are positive constants then $\lambda_1 > 1$. Hence the equilibrium point E_2 is a saddle point.

At E_3 the Jacobian matrix J takes the form as shown in Eq. 3.6:

$$J(E_3) = \begin{bmatrix} 1-\frac{Vc_2\alpha_1}{W} & -\frac{\alpha_1 \beta k c_2}{W} & -\frac{\alpha_1 W \mu c_2}{W} \\ 0 & 1+\alpha_2 k\left(\varphi - c_1 + \beta\frac{c_2}{W}\right) & 0 \\ \frac{\alpha_3(UW - Vc_2)}{W} & 0 & 1 \end{bmatrix} \tag{3.6}$$

one of whose eigenvalues is $\lambda = 1+\alpha_2 k\left(\varphi - c_1 + \beta\frac{c_2}{W}\right)$. Since α_2, k, $(\varphi - c_1)W + c_2\beta$ are positive constants then $\lambda > 1$. Hence the equilibrium point E_3 is a saddle point.

At E_4 the Jacobian matrix J takes the form as shown in Eq. 3.7:

$$J(E_4) = \begin{bmatrix} 1+\alpha_1(U - 2Vx - \beta k y) & -x\alpha_1\beta k & -x\alpha_1 W\mu \\ \alpha_2 k\beta y & 1+\alpha_2[k(\varphi - c_1 + \beta x) - 4by] & 0 \\ 0 & 0 & 1+\alpha_3(Wx - c_2) \end{bmatrix} \tag{3.7}$$

one of whose eigenvalues is $= 1+\alpha_3\left(W\frac{2bU-\beta k^2(\varphi - c_1)}{2bV+\beta^2 k^2} - c_2\right) = 1+\alpha_3\frac{2b(WU-Vc_2)-\beta k^2[(\varphi - c_1)W+c_2\beta]}{2bV+\beta^2 k^2}$. Since α_3, $2bV+\beta^2 k^2$, $2b(WU - Vc_2) - \beta k^2[(\varphi - c_1)W + c_2\beta]$ are positive constants then $\lambda > 1$. Hence the equilibrium point E_4 is a saddle point.

Lemma 2. *The boundary equilibrium point E_* of the system (2.4) is locally asymptotically stable provided that $(\varphi - c_1)W + c_2\beta > 0$, $2b(WU - Vc_2) - \beta k^2[(\varphi - c_1)W + c_2\beta] > 0$, and the Jury stability criterion (Necessary and sufficient condition for the local stability of Nash equilibrium) are satisfied.*

Proof. To prove this result, we estimate the Jacobian matrix J at E_*, which takes the form as shown in Eq. 3.8:

$$J(E_*) = \begin{bmatrix} 1-\alpha_1 V x^* & -\alpha_1\beta k x^* & -\alpha_1 W\mu x^* \\ \alpha_2 k\beta y^* & 1-2\alpha_2 b y^* & 0 \\ \alpha_3\mu W z^* & 0 & 1 \end{bmatrix} \tag{3.8}$$

whose eigenvalues are λ_1, λ_2 and λ_3. The characteristic polynomial is given by Eq. 3.9

$$f(\lambda) = \lambda^3 + a_2\lambda^2 + a_1\lambda + a_0 \tag{3.9}$$

where

$$\begin{cases} a_2 = -trJ(E_5) = -3 + \alpha_1 V x^* + 2\alpha_2 b y^* \\ a_1 = \alpha_1\alpha_3\mu^2 W^2 x^* z^* + (1 - \alpha_1 V x^*)(1 - 2\alpha_2 b y^*) + \alpha_1\alpha_2 k^2\beta^2 x^* y^* + 2 - \alpha_1 V x^* - 2\alpha_2 b y^* \\ a_0 = -detJ(E_5) = \alpha_1\alpha_3\mu^2 W^2 x^* z^*(2\alpha_2 b y^* - 1) - (1 - \alpha_1 V x^*)(1 - 2\alpha_2 b y^*) - \alpha_1\alpha_2 k^2\beta^2 x^* y^* \end{cases} \tag{3.10}$$

Denote $b_k = \begin{vmatrix} a_0 & a_{3-k} \\ a_3 & a_k \end{vmatrix}, k = 0,1,2$. The necessary and sufficient conditions for the local stability of equilibrium points of a 3-dimensional discrete dynamic system are given by the Jury stability criterion as shown in Eq. 3.11:

$$\begin{gathered} (\mathrm{i}) f(1) > 0 \\ (\mathrm{ii})(-1)^n f(-1) > 0 \\ (\mathrm{iii})|a_0| < a_n \\ (\mathrm{iv})|b_0| > |b_{n-1}| \end{gathered} \tag{3.11}$$

Then the following statements are held in Eq. 3.12:

$$\begin{gathered} (\mathrm{i})\ |a_0| < 1 \\ (\mathrm{ii})\ a_2 + a_1 + a_0 > -1 \\ (\mathrm{iii})\ a_2 - a_1 + a_0 < 1 \\ (\mathrm{iv})|{a_0}^2 - 1| > |a_2 a_0 - a_1| \end{gathered} \tag{3.12}$$

From these results, we obtain information on both the stability region and the impacts of the model parameters on the locally asymptotical stability of the Nash equilibrium point E_*. For instance, an increment of the speed of adjustment of a boundedly rational player with the other parameters held fixed, has a destabilizing effect. An increase of $\alpha_1, \alpha_2\ and\ \alpha_3$ can bring the original equilibrium point out of the stability region. Simultaneously, the change in other major parameters in the model can also cause the loss of stability of E_*. Complex dynamic behaviors such as chaos occur where the parameters go beyond the stability region and the maximum Lyapunov exponents of the system become positives. Through numerical simulations, the impacts of major parameters on the local stability of the 3-dimensional system (2.4) will be investigated respectively in the next chapter.

4. Numerical Simulations

The main aim is to analyze the impacts of the adjustment speed, the ecological compensation policies, and the environmental tax policy on the dynamic behaviors of players with bounded rationality. Various numerical experiments were simulated to manifest the chaoticity of the 3-dimensional system (2.4). Numerical evidence including bifurcations diagrams, strange attractors, Lyapunov exponents, sensitive dependence on initial conditions was provided here. To study the local stability properties of the equilibrium points, it is convenient to take the values of the parameters as follows: $\sigma = 1,\ \beta = 1.5,\ a = 10,\ b = 3,\ \omega = 1,\ k = 0.9,\ c_1 = 0.5,\ \varphi = 4,\ s = 0.8,\ t_1 = 0.1,\ t_2 = 0.2,\ t_3 = 0.4,\ \rho = 0.3,\ \mu = 10,\ P = 100,\ e = 0.7,\ \theta = 1,\ \gamma = 0.5,\ c_2 = 0.2$, where the Nash equilibrium point is computed as $E_* = (x^*, y^*, z^*) = (0.2857, 0.5893, 0.1496)$.

Figure 1 shows the graph of the strange attractor for $\alpha_1 = 0.7,\ \alpha_2 = 0.5,\ \alpha_3 = 0.5$ where the Nash equilibrium point E_* is locally stable. A strange attractor is a set of states with a fractal structure towards which a system tends to evolve for a wide variety of initial conditions. As is depicted in the diagram, while $(\alpha_1, \alpha_2, \alpha_3)$ is within the stability region and the system remains locally stable, the dynamical behaviors of the boundedly rational players exhibit a spiral trajectory that converges to the Nash equilibrium point E_*.

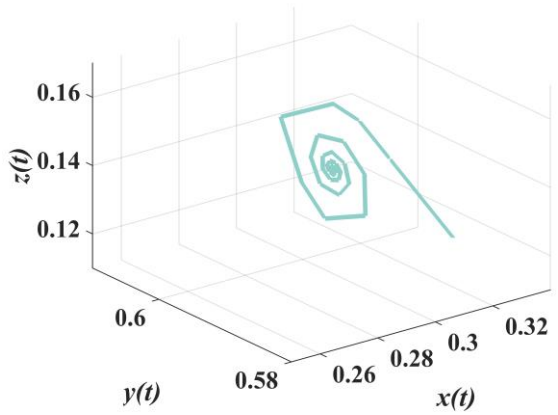

Figure 1: The strange attractor for $\alpha_1 = 0.7,\ \alpha_2 = 0.5,\ \alpha_3 = 0.5$

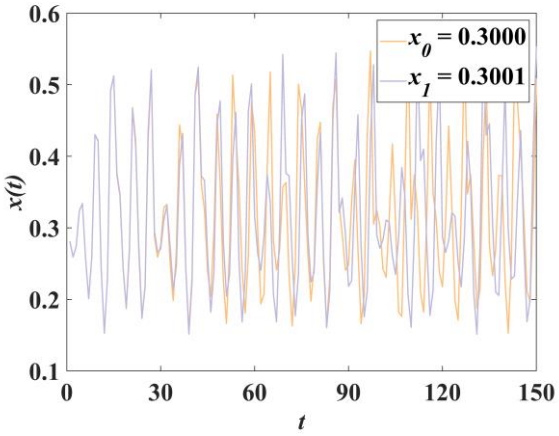

Figure 2: Sensitive dependence on initial conditions, parameter values $(\alpha_1, \alpha_2, \alpha_3) = (1, 0.22, 0.9)$ and initial conditions (x_0, y_0, z_0) and $(x_0 + 0.0001, y_0, z_0)$

As the speed of adjustment increases, the dynamic system evolves into a chaotic state. To demonstrate the sensitivity to initial conditions, two orbits with initial points which differ by 0.0001 are computed respectively. Figures 2-4 exhibit sensitive dependence on initial conditions with the parameter values $(\alpha_1, \alpha_2, \alpha_3) = (1, 0.22, 0.9)$ beyond the stability region of the equilibrium point. As is vividly illustrated in the diagrams, at the beginning the time series appear difficult to be identified; nevertheless, the distinction between two orbits builds up rapidly after multiple iterations.

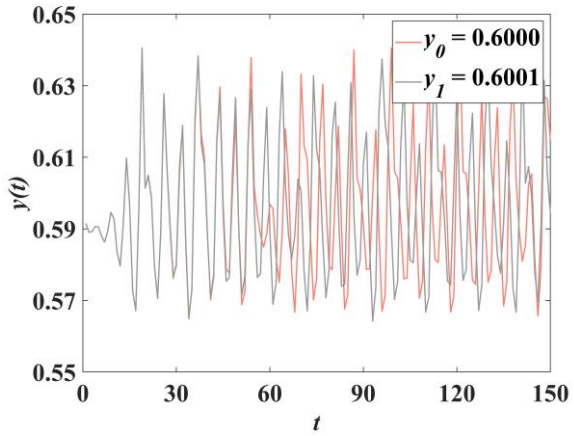

Figure 3: Sensitive dependence on initial conditions, parameter values $(\alpha_1, \alpha_2, \alpha_3) = (1, 0.22, 0.9)$ and initial conditions (x_0, y_0, z_0) and $(x_0 + 0.0001, y_0, z_0)$

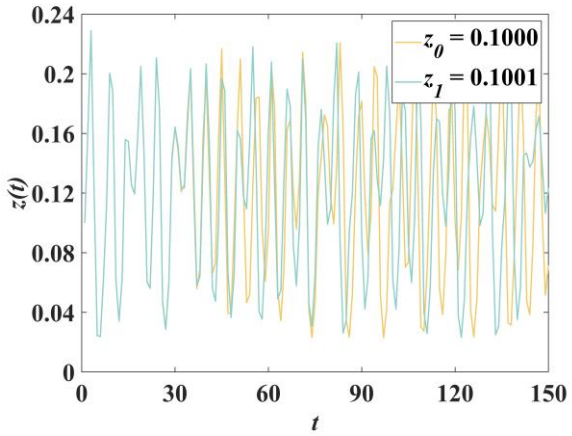

Figure 4: Sensitive dependence on initial conditions, parameter values $(\alpha_1, \alpha_2, \alpha_3) = (1, 0.22, 0.9)$ and initial conditions (x_0, y_0, z_0) and $(x_0, y_0 + 0.0001, z_0)$

From Figure 2-4, it is evident that the time series of the system (2.4) show sensitive dependence to initial conditions, hence complex dynamics behaviors occur in the 3-player model. As a consequence, the occurrence of chaos makes it impracticable to make predictions correctly and implement policies efficaciously for local governments, peasant households, and polluting enterprises in reality. Hence, it is essential to analyze the impacts of major parameters such as the adjustment speed of a boundedly rational player on the local stability of the system (2.4).

4.1. Impacts of the Adjustment Speed on the System

4.1.1 Adjustment Speed of Local Governments

The bifurcation diagram concerning the adjustment speed of local governments α_1 for $\alpha_2 = 0.2,\ \alpha_3 = 0.15$ is shown in Figure 5. The maximal Lyapunov exponent depending on α_1 is also plotted to detect the occurrences of bifurcation and chaos. For discrete-time system $x_{n+1} = f(x_n)$, for an orbit that starts with x_0, the maximal Lyapunov exponent can be defined by the Eq. 4.1:

$$\lambda(x_0) = \lim_{n\to\infty} \frac{1}{n} \sum_{i=o}^{n-1} \ln|f'(x_i)| \tag{4.1}$$

For $\alpha_1 < 1.9$, while the maximal Lyapunov exponent is below zero, the Nash equilibrium point E_* maintains locally stable and insensitive to initial conditions (Figure 5). With the increase of α_1, the equilibrium point E_* loses stability gradually, and complex dynamic behaviors such as period-doubling bifurcation and chaotic behavior were observed. For $\alpha_1 = 1.9$, while the maximal Lyapunov exponent reaches zero, the system converges to a period-doubling bifurcation. While the maximal Lyapunov exponent rises above zero, the system evolves into a chaotic state.

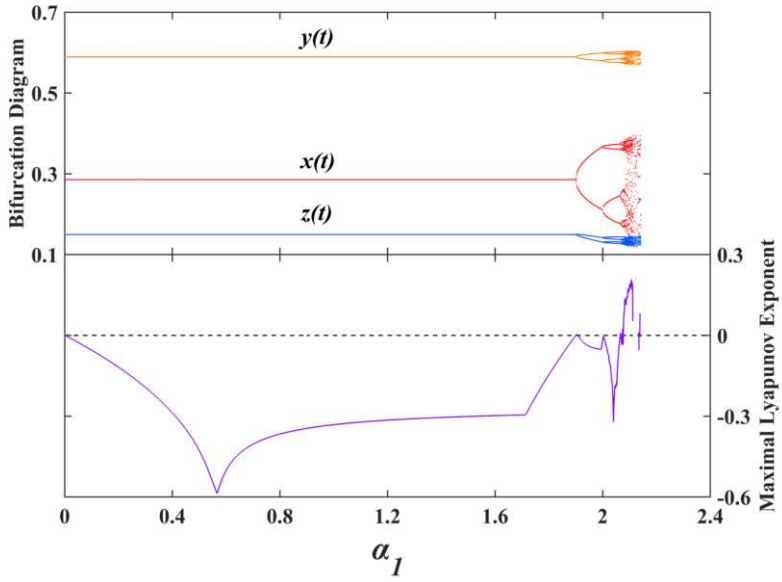

Figure 5: Bifurcation diagram and maximal Lyapunov exponent concerning α_1 for $\alpha_2 = 0.2,\ \alpha_3 = 0.15$

Figures 6-7 show the graph of strange attractors for $\alpha_2 = 0.2,\ \alpha_3 = 0.15$. With the increase of the adjustment speed α_1, the originally stable point begins to appear as a branch state for $\alpha_1 = 1.9$, and eventually enters into a chaotic state for $\alpha_1 = 2.08$. The dynamic system with a chaotic attractor is locally unstable yet globally stable: subject to the confines of the attractor, any arbitrary close initial points on the attractor diverge from each other after various iterations but never depart from the attractor.

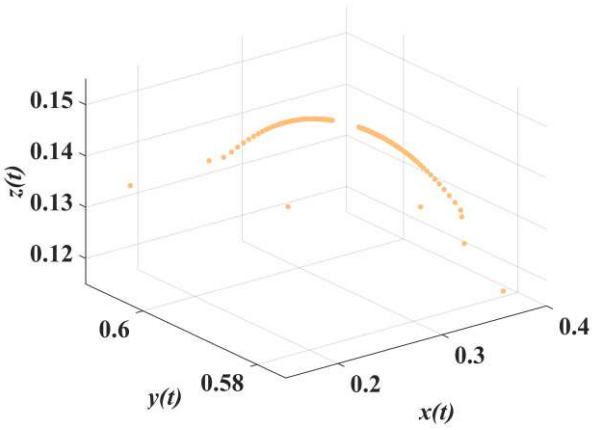

Figure 6: The strange attractor for $\alpha_1 = 1.9,\ \alpha_2 = 0.2,\ \alpha_3 = 0.15$

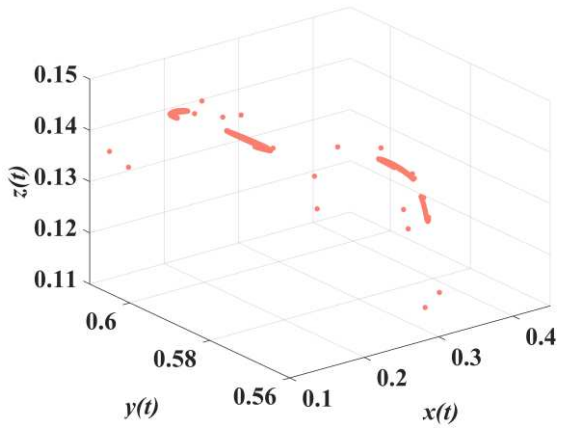

Figure 7: The strange attractor for $\alpha_1 = 2.08,\ \alpha_2 = 0.2,\ \alpha_3 = 0.15$

4.1.2 Adjustment Speed of Peasant Households

The bifurcation diagram and maximal Lyapunov exponent concerning the adjustment speed of peasant households α_2 for $\alpha_1 = 0.7,\ \alpha_3 = 0.5$ is shown in Figure 8. While $\alpha_2 < 0.59$, the maximal Lyapunov exponent remains negative, and the Nash equilibrium point E_* is locally stable and insensitive to initial conditions. As α_2 increases to 0.59, the equilibrium point E_* becomes unstable, and complex dynamic phenomena begin to occur, including period-doubling bifurcation and finally chaotic behavior. It can be observed that when the maximal Lyapunov exponent reaches zero, the system enters a period-doubling bifurcation. When the maximal Lyapunov exponent is positive, complex chaotic behaviors begin to appear.

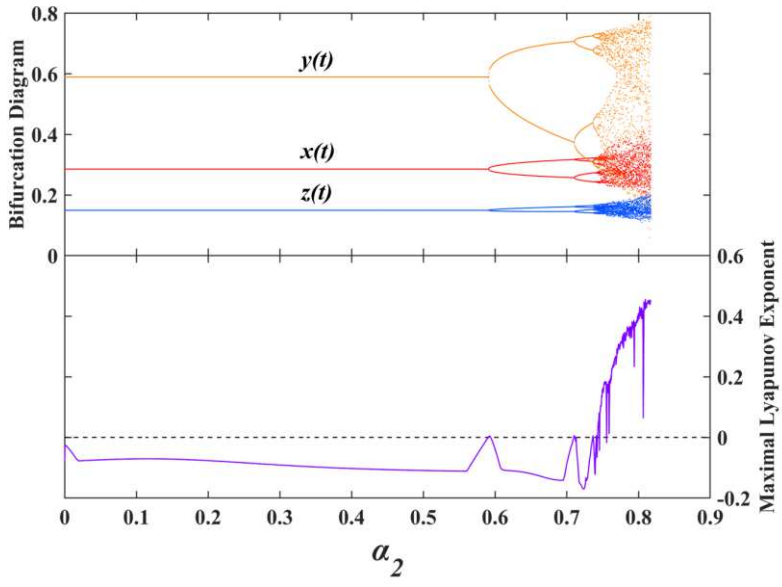

Figure 8: Bifurcation diagram and maximal Lyapunov exponent concerning α_2 for $\alpha_1 = 0.7,\ \alpha_3 = 0.5$

Figures 9-10 show the graph of strange attractors for $\alpha_1 = 0.7,\ \alpha_3 = 0.5$. In marked contrast to the unchaotic attractor plotted in Figure 1, as the adjustment speed α_2 increases to 0.59, the strange attractor revolves from the Nash equilibrium point into a period-doubling bifurcation. Complex chaotic phenomena ultimately occur for $\alpha_2 = 0.8$, where the attractor shows sensitive dependence on initial conditions, and arbitrarily nearby points will deviate

from each other once some sequences have entered the strange attractor.

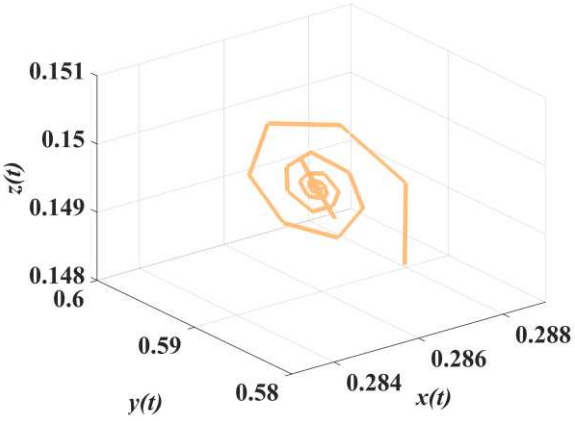

Figure 9: The strange attractor for $\alpha_1 = 0.7,\ \alpha_2 = 0.59,\ \alpha_3 = 0.5$

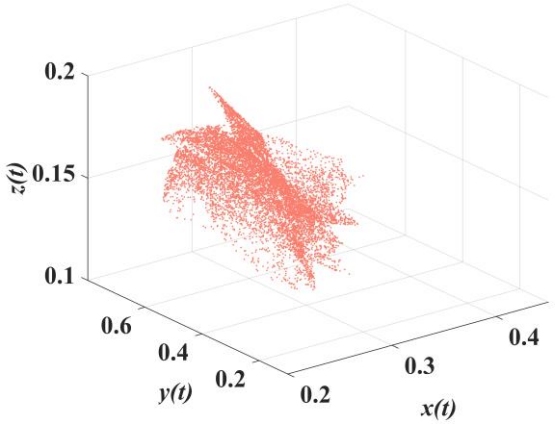

Figure 10: The strange attractor for $\alpha_1 = 0.7,\ \alpha_2 = 0.8,\ \alpha_3 = 0.5$

4.1.3 Adjustment Speed of Polluting Enterprises

The bifurcation diagram and maximal Lyapunov exponent for the adjustment speed of polluting enterprises α_3 for $\alpha_1 = 1,\ \alpha_2 = 0.22$ was found (Figure 11). As is exhibited in the diagram, while the maximal Lyapunov exponent is negative, the Nash equilibrium point E_* maintains locally stable and insensitive to initial conditions. With the increase of α_3, the equilibrium point E_* loses stability gradually, and complex dynamic behaviors such as period-doubling bifurcation and chaotic behavior were observed.

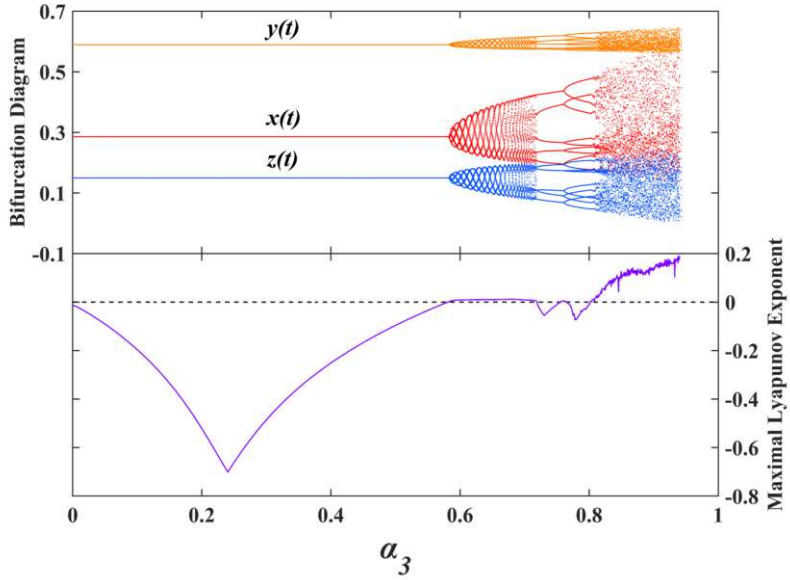

Figure 11: Bifurcation diagram and maximal Lyapunov exponent concerning α_3 for $\alpha_1 = 1,\ \alpha_2 = 0.22$

Figures 12-13 show the graph of strange attractors for $\alpha_1 = 1,\ \alpha_2 = 0.22$. As the adjustment speed α_3 increases, the strange attractor goes through a period-doubling bifurcation for $\alpha_3 = 0.76$. Chaos finally occurs for $\alpha_3 = 0.9$, where the attractor appears in a complex fractal state and the dynamic system becomes very unstable.

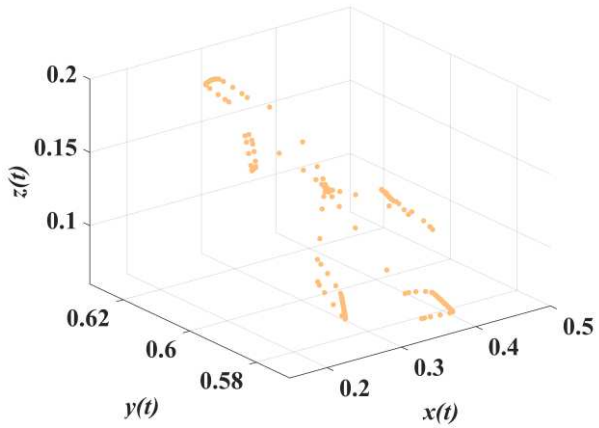

Figure 12: The strange attractor for $\alpha_1 = 1,\ \alpha_2 = 0.22,\ \alpha_3 = 0.76$

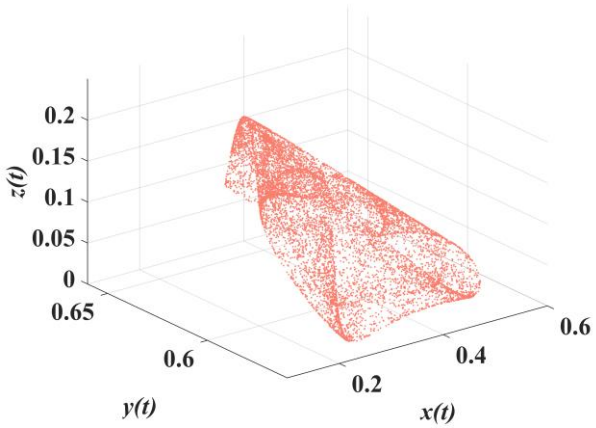

Figure 13: The strange attractor for $\alpha_1 = 1,\ \alpha_2 = 0.22,\ \alpha_3 = 0.9$

4.2 Influences of the Ecological Compensation Policies on the System

To encourage green production, the ecological compensation policies made by local governments have profound impacts on the decision-making of farmer households and polluting enterprises. With the change of ecological compensations, the policy implementation intensity varies. The influences of ecological compensation policies on the dynamical behaviors of the system were discussed in this study.

4.2.1 Ecological Compensation Policy for Peasant Households

Figure 14 shows the bifurcation diagrams concerning the ecological compensation for peasant households. As is depicted in Figure 14 (a), where the original system is locally stable with the parameter values $(\alpha_1, \alpha_2, \alpha_3) = (0.7, 0.5, 0.5)$, chaotic behavior is observed for the small values of the parameter β. An increment of the ecological compensation β has a stabilizing effect and restores the stability of the system (2.4). Simultaneously, the peasant households' agricultural output at the equilibrium point is significantly enlarged. Nevertheless, the polluting enterprises' treatment intensity of nitrogenous decreases to zero for $\beta = 2.3$, indicating that polluting enterprises become reluctant to cooperate while the ecological compensation for peasant households is inappropriately large.

The bifurcation diagram where the system (2.4) is in a chaotic state due to the increase of adjustment speed of local governments is shown in Figure 14 (b). It is manifested that an increment of the parameter β can effectively stabilize the dynamic system (4.2) and enlarge peasant households' agricultural output. Nevertheless, bifurcation and chaos reemerge when the ecological compensation coefficient β is too large.

The bifurcation diagram where the system is in a chaotic state due to the increase of adjustment speed of peasant households is shown in Figure 14 (c). It is demonstrated that the system remains chaotic for the small values of the parameter β when the adjustment speed of peasant households is beyond the stability region. The actual cause accounting for the phenomenon is that peasant households' exceptionally quick speed of adjusting agricultural output exerts intricate impacts on other stakeholders, causing the dynamic system to become extremely unstable.

The bifurcation diagram where the system is in a chaotic state due to the increment of adjustment speed of polluting enterprises is shown in Figure 14 (d). The dynamical behaviors of the system resemble that in Figure 14 (a). Hence, an increase of the ecological compensation β can stabilize the system and enlarge agricultural output, yet polluting enterprises' treatment intensity of nitrogenous pollutants will be substantially compromised.

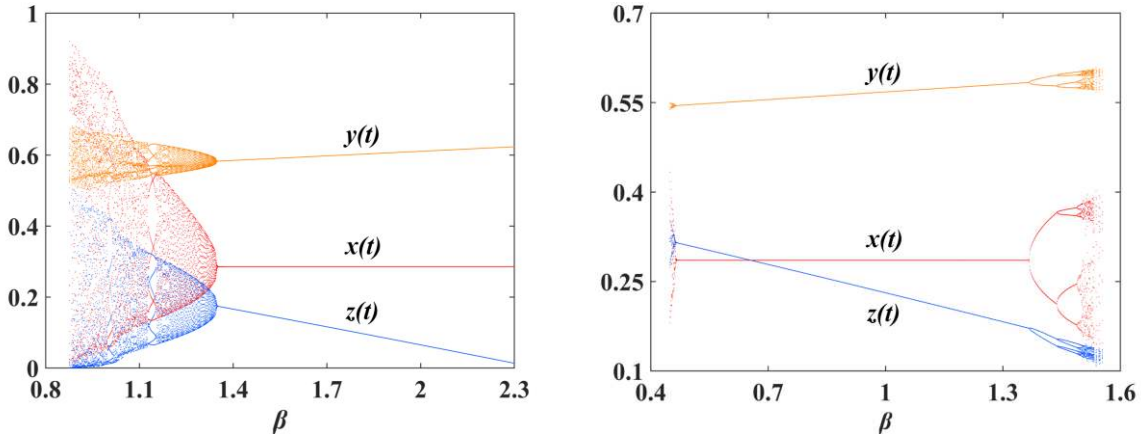

(a) $\alpha_1 = 0.7,\ \alpha_2 = 0.5,\ \alpha_3 = 0.5$ (b) $\alpha_1 = 2.08,\ \alpha_2 = 0.2,\ \alpha_3 = 0.15$

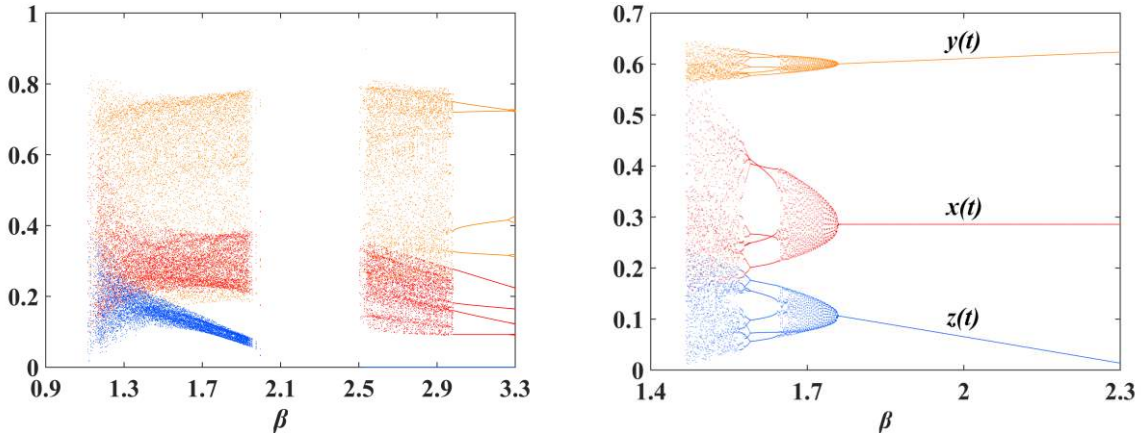

(c) $\alpha_1 = 0.7,\ \alpha_2 = 0.8,\ \alpha_3 = 0.5$ (d) $\alpha_1 = 1,\ \alpha_2 = 0.22,\ \alpha_3 = 0.9$

Figure 14: Bifurcation diagram for β

4.2.2 Ecological Compensation Policy for Polluting Enterprises

Figure 15 shows the bifurcation diagrams concerning the ecological compensation for polluting enterprises. As is demonstrated in Figure 15 (a), where the original system is locally stable with the parameter values $(\alpha_1, \alpha_2, \alpha_3) = (0.7, 0.5, 0.5)$, the equilibrium point remains stable for the small values of the parameter ρ. With the increment of ecological compensation for polluting enterprises, local governments' policy implementation intensity and peasant households' agricultural output drop dramatically, whereas polluting enterprises' treatment intensity of nitrogenous pollutants slightly increases. The system revolves into a chaotic state when the ecological compensation ρ is too large, inhibiting decision-makers from making optimal strategies.

Figure 15 (b) shows the bifurcation diagram where the system is in a chaotic state due to the increase of adjustment speed of local governments. It is vivid that an appropriate increase of the parameter ρ has a stabilizing effect. Moreover, local governments' policy implementation intensity, peasant households' agricultural output, and polluting enterprises' treatment intensity of nitrogenous pollutants at the equilibrium point will all be reduced. When the ecological compensation ρ is too large, the reappearance of chaos is exhibited in the diagram.

Figure 15 (c) shows the bifurcation diagram where the system is in a chaotic state due to the increase of adjustment speed of peasant households. It is indicated that the dynamic system concerning the ecological compensation for polluting enterprises remains chaotic with the adjustment speed of peasant households beyond the stability region.

Figure 15 (d) shows the bifurcation diagram where the system is in a chaotic state due to the increase of adjustment speed of polluting enterprises. The dynamical behaviors of the system resemble that in Figure 15 (a). Therefore, a moderate increment of the ecological compensation ρ will restore the local stability of the system.

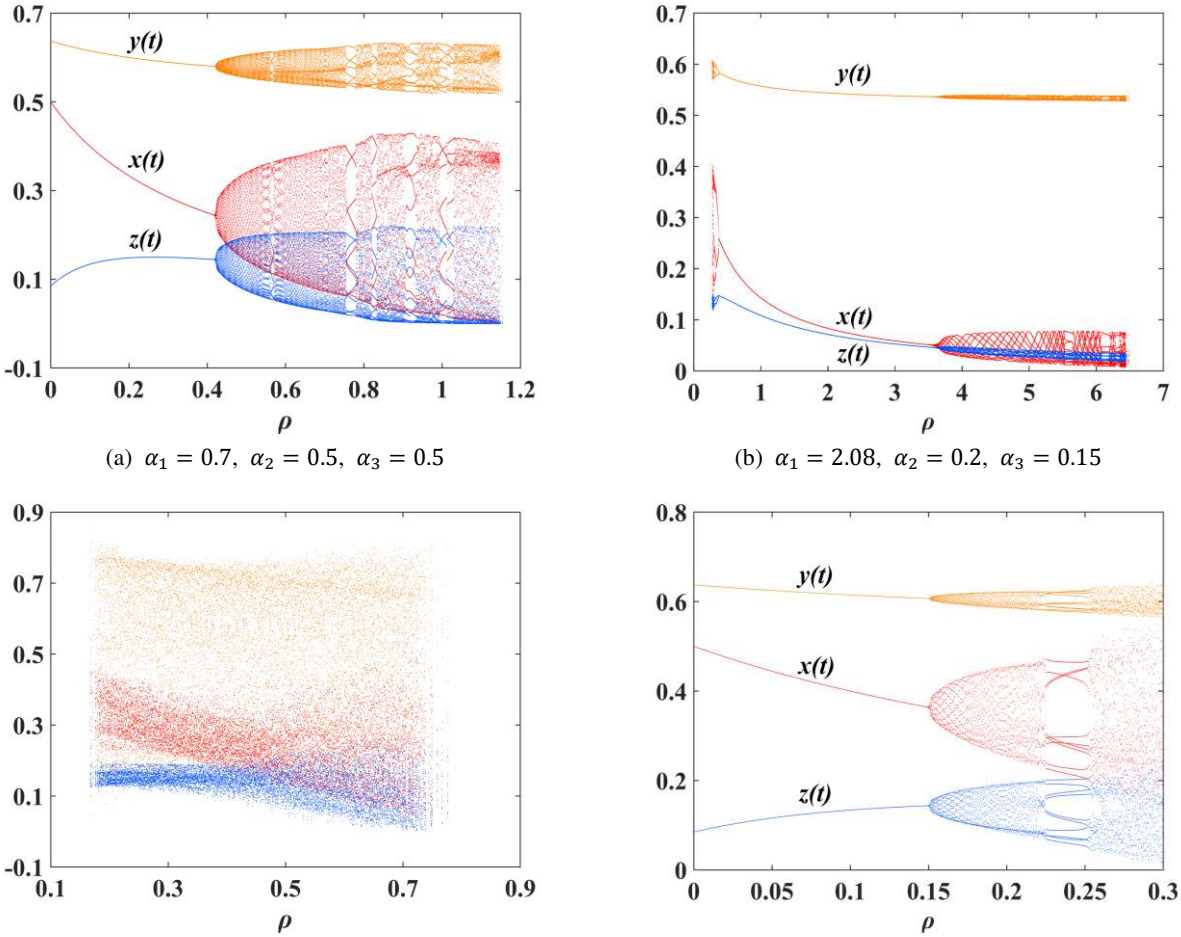

(a) $\alpha_1 = 0.7,\ \alpha_2 = 0.5,\ \alpha_3 = 0.5$ (b) $\alpha_1 = 2.08,\ \alpha_2 = 0.2,\ \alpha_3 = 0.15$

(c) $\alpha_1 = 0.7,\ \alpha_2 = 0.8,\ \alpha_3 = 0.5$ (d) $\alpha_1 = 1,\ \alpha_2 = 0.22,\ \alpha_3 = 0.9$

Figure 15: Bifurcation diagram for ρ

4.3 Effects of the Environmental Tax Policy on the System

The environmental tax policy, which can be envisaged as a penalty mechanism, urges polluting enterprises to enhance the treatment intensity of nitrogenous pollutants. To set an appropriate environmental tax rate, it is vital to investigate its impacts on the local stability of the system (2.4).

Figure 16 shows the bifurcation diagrams for the environmental tax rate t_3. As is illustrated in Figure 16 (a), where the system is locally stable with the parameter values $(\alpha_1, \alpha_2, \alpha_3) = (0.7, 0.5, 0.5)$, the equilibrium point is locally stable for the small values of the parameter t_3. With the increase of environmental tax rate, local governments' policy implementation intensity and peasant households' agricultural output decline marginally, whereas polluting enterprises' treatment intensity of nitrogenous pollutants significantly increases. Chaotic behaviors of the dynamical system are detected when the environmental tax rate is set too high.

Figure 16 (b) shows the bifurcation diagram where the system is in a chaotic state due to the increase of adjustment speed of local governments. It is depicted that bifurcation and chaos first occur with an increase of the parameter t_3. Then, the system is stabilized at the equilibrium point where local governments' policy implementation intensity and peasant households' agricultural output are reduced while polluting enterprises'

treatment intensity of nitrogenous pollutants is notably enhanced. When the environmental rate is too high, the dynamic system loses stability and revolves into a chaotic state again.

Figure 16 (c) shows the bifurcation diagram where the system is in a chaotic state due to the increase of adjustment speed of peasant households. It is revealed that the dynamic system concerning the environmental tax rate is very unstable while the adjustment speed of peasant households is beyond the stability region.

Figure 16 (d) shows the bifurcation diagram where the system is in a chaotic state due to the increase of adjustment speed of polluting enterprises. The dynamical behaviors of the system appear similar to that in Figure 16 (a). Therefore, a proper increment of the environmental tax rate will restore the local stability of the system.

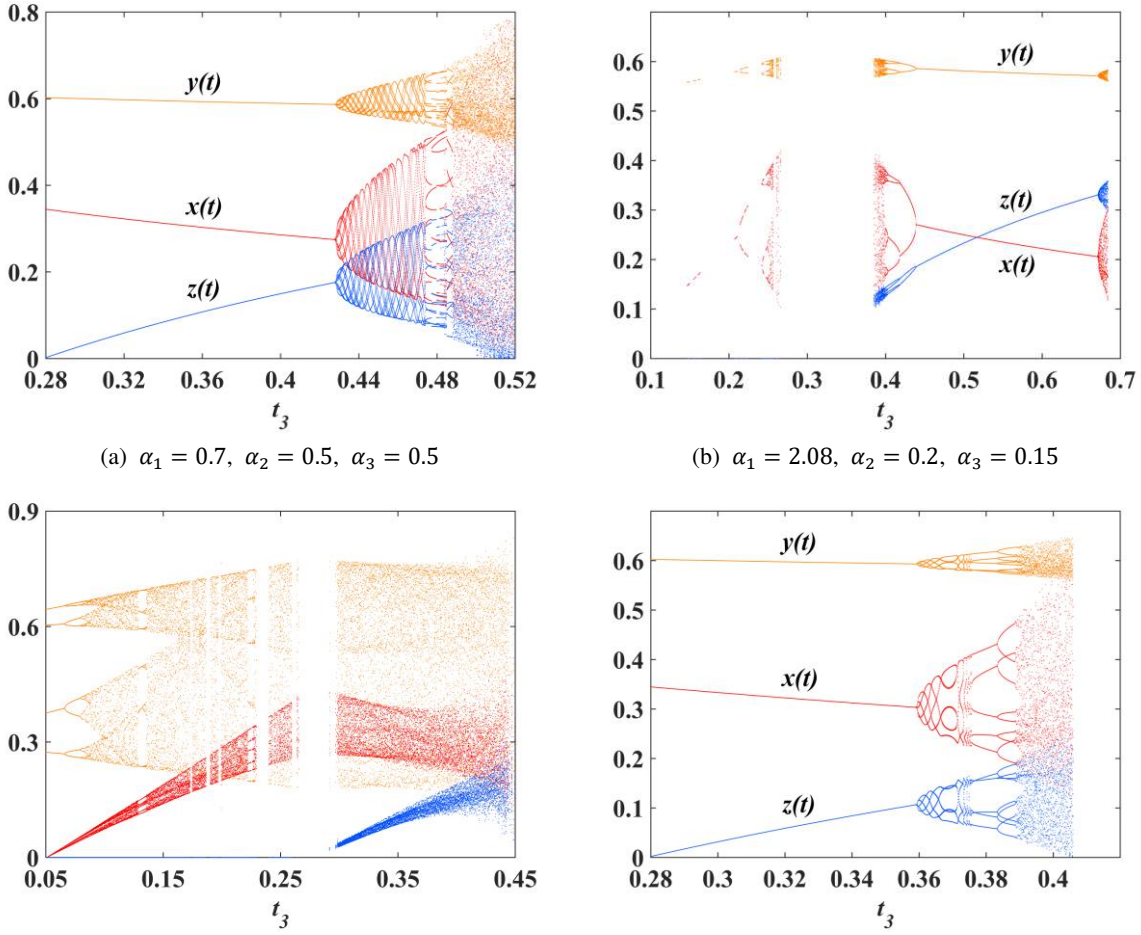

(a) $\alpha_1 = 0.7,\ \alpha_2 = 0.5,\ \alpha_3 = 0.5$ (b) $\alpha_1 = 2.08,\ \alpha_2 = 0.2,\ \alpha_3 = 0.15$

(c) $\alpha_1 = 0.7,\ \alpha_2 = 0.8,\ \alpha_3 = 0.5$ (d) $\alpha_1 = 1,\ \alpha_2 = 0.22,\ \alpha_3 = 0.9$

Figure 16: Bifurcation diagram for t_3

5. Control of Chaos

Numerical simulations have proven that an increase in the adjustment speed of a boundedly rational player has a destabilizing effect. While the dynamical system loses stability and evolves into a chaotic state, the players are incapable of making optimal strategies. Hence, it is advisable to perform chaos control in the maintenance of the local stability of the dynamic system. In this study, we adopt the delayed feedback control scheme to eliminate chaos.

The delayed feedback control scheme realizes chaos control by introducing a feedback controller while the parameters of the system are held fixed. The controller with a simple structure has certain robustness to minor

disturbances. The delayed feedback control scheme proposed by Pyragas [20] is as follows:

$$u(t) = k[y(t+1-\tau) - y(t+1)], t > \tau \tag{5.1}$$

where the length of time delay is denoted as τ. By substituting $\tau = 1$ into the third equation of the system (2.4), the controlled system stabilized at the equilibrium point E_* is as follows:

$$\begin{cases} x(t+1) = x(t)\left[1 + \alpha_1\left(U - Vx(t) - \beta k y(t) - W\mu z(t)\right)\right] \\ y(t+1) = y(t)\left\{1 + \alpha_2\left[k\left(\varphi - c_1 + \beta x(t)\right) - 2by(t)\right]\right\} \\ z(t+1) = z(t)\left[1 + \dfrac{\alpha_3}{k_1+1}\mu(Wx(t) - c_2)\right] \end{cases} \tag{5.2}$$

where k_1 is denoted as a positive feedback controller. The Jacobian matrix J' at E_* takes the form:

$$J'(E_*) = \begin{bmatrix} 1 - \alpha_1 V x^* & -\alpha_1 \beta k x^* & -\alpha_1 W \mu x^* \\ \alpha_2 k \beta y^* & 1 - 2\alpha_2 b y^* & 0 \\ \dfrac{\alpha_3 \mu W z^*}{k_1+1} & 0 & 1 + \dfrac{\alpha_3}{k_1+1}\mu(Wx(t) - c_2) \end{bmatrix} \tag{5.3}$$

whose eigenvalues are λ_1, λ_2 and λ_3. The characteristic polynomial is given by

$$f(\lambda) = \lambda^3 + a_2'\lambda^2 + a_1'\lambda + a_0'$$

The local stability conditions of the equilibrium point are given by recalling Jury's conditions which are the necessary and sufficient conditions for the system (5.1) to converge to the equilibrium point $E_* = (x^*, y^*, z^*)$. Then the following statements are held:

$$\begin{gathered} \text{(i) } |a_0'| < 1 \\ \text{(ii) } a_2' + a_1' + a_0' > -1 \\ \text{(iii) } a_2' - a_1' + a_0' < 1 \\ \text{(iv)} |a_0'^2 - 1| > |a_2' a_0' - a_1'| \end{gathered} \tag{5.4}$$

From equation (5.4) we obtain information on the stability region and bifurcation curve of the controlled system (5.2). With the increment of the feedback controller k_1, the destabilizing effect caused by the increase of adjustment speed of polluting enterprises can be eliminated by control of chaos. Numerical experiments are simulated to demonstrate the efficiency of the chaos control scheme. It is convenient to take $\alpha_1 = 1$, $\alpha_2 = 0.22$, $\alpha_3 = 0.9$, where the original dynamic system (2.4) is in chaos because the adjustment speed of polluting enterprises is too large.

Figures 17-18 show the bifurcation diagram and maximal Lyapunov exponent of the controlled system (5.2) concerning the feedback controller k_1. As is illustrated in the diagram, for $k_1 < 0.54$, the maximal Lyapunov exponent is beyond zero, and complex dynamical behaviors such as bifurcation and chaos are observed. While $k_1 > 0.54$, the maximal Lyapunov exponent is negative, and the system (5.2) is stabilized at the equilibrium point E_*. The results prove that an increment of the feedback controller k_1 can eliminate chaos and restore stability.

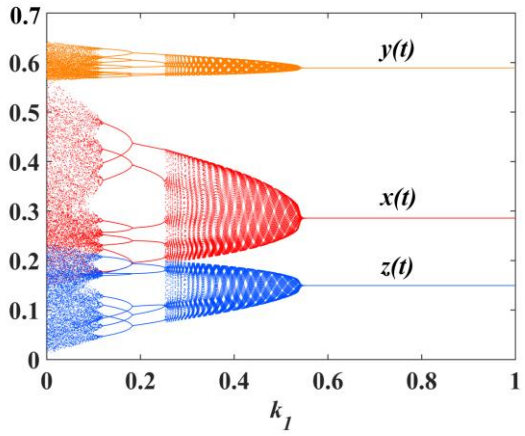

Figure 17: Bifurcation diagram for k_1

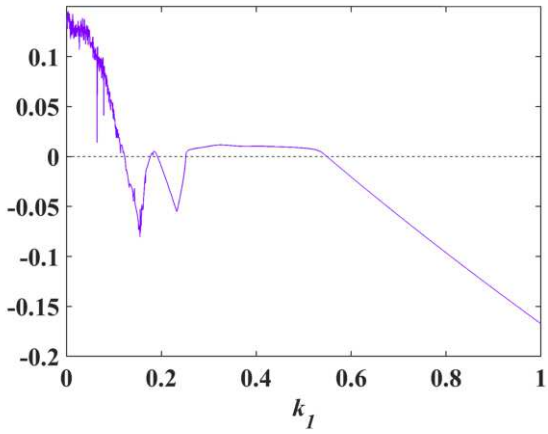

Figure 18: Maximal Lyapunov exponent for k_1

6. Conclusions

To enhance N utilization efficiency, this study aims to integrate ecological compensation and environmental tax policies by investigating the dynamic behaviors of decision-makers in the N cascade. Firstly, we proposed and analyzed the dynamical behaviors of a 3-player game model, which contains boundedly rational players: local governments, peasant households, and polluting enterprises with bounded rationality. Then, the Nash equilibrium points and local stability of the dynamical systems are investigated. Furthermore, numerical simulations are rendered to manifest that, complex dynamical behaviors such as bifurcation and chaos arise from the variation of some parameters of the model. It is proven that the fast adjustment can cause the market structure to behave chaotically, whereas appropriate ecological compensation and environmental tax policies can restore the stability of the system. Additionally, in an endeavor to eliminate chaos and achieve a stable market, chaos control of the dynamic systems is discussed using the delayed feedback control scheme.

Research results indicate that a moderate increment of the ecological compensation for peasant households can generally restore stability and enlarge agricultural output, though polluting enterprises' treatment intensity is bound to be compromised. Meanwhile, in terms of the ecological compensation for polluting industries, the market will only remain stable when the adjustment speed of peasant households lies within the stability region. Moreover, environmental tax increase must be on a small scale to enhance treatment intensity and avoid chaos.

References

[1] Kanter D R, Zhang X, Mauzerall D L.: Reducing nitrogen pollution while decreasing farmers' costs and increasing fertilizer industry profits. Journal of environmental quality. 44(2), 325-335 (2015)

[2] Sutton M A, Howard C M, Kanter D R, et al.: The nitrogen decade: mobilizing global action on nitrogen to 2030 and beyond. One Earth. 4(1), 10-14 (2021)

[3] Ghosh B C, Bhat R.: Environmental hazards of nitrogen loading in wetland rice fields. Environmental pollution. 102(1), 123-126. (1998)

[4] Howarth R W.: The development of policy approaches for reducing nitrogen pollution to coastal waters of the USA. Science in China Series C: Life Sciences. 48(2), 791-806 (2005)

[5] Presterl T, Groh S, Landbeck M, et al.: Nitrogen uptake and utilization efficiency of European maize hybrids developed under conditions of low and high nitrogen input. Plant Breeding. 121(6), 480-486 (2002)

[6] Das S, Ghose M, Spooner-Hart R.: Effects of salinity on photosynthesis, leaf anatomy, ion accumulation and photosynthetic nitrogen use efficiency in five Indian mangroves. Wetlands Ecology and Management. 15(4), 347-357 (2007)
[7] Dukes E S M, Galloway J N, Band L E, et al.: A community nitrogen footprint analysis of Baltimore City, Maryland. Environmental Research Letters. 15(7), 75-77 (2020)
[8] Galloway J N, Winiwarter W, Leip A, et al.: Nitrogen footprints: past, present and future. Environmental Research Letters. 9(11), 115-119 (2014)
[9] Tanaka H, Kyaw K M, Toyota K, et al.: Influence of application of rice straw, farmyard manure, and municipal biowastes on nitrogen fixation, soil microbial biomass N, and mineral N in a model paddy microcosm. Biology and fertility of soils. 42(6), 501-505 (2006)
[10] Cole M A.: US environmental load displacement: examining consumption, regulations and the role of NAFTA. Ecological economics. 48(4), 439-450 (2004)
[11] Gao X, Shen J, He W, et al.: An evolutionary game analysis of governments' decision-making behaviors and factors influencing watershed ecological compensation in China. Journal of Environmental Management. 251, 109-112 (2019)
[12] Shen J, Gao X, He W, et al.: Prospect theory in an evolutionary game: Construction of watershed ecological compensation system in Taihu Lake Basin. Journal of Cleaner Production. 291, 125-129 (2021)
[13] Bárcena-Ruiz J C.: Environmental taxes and first-mover advantages. Environmental and Resource Economics. 35(1), 19-39 (2006)
[14] Jørgensen S.: A dynamic game of waste management. Journal of Economic Dynamics and Control. 34(2), 258-265 (2010)
[15] Bischi G I, Naimzada A.: Global analysis of a dynamic duopoly game with bounded rationality. Advances in dynamic games and applications. 13, 361-385 (2020)
[16] Puu T.: Chaos in duopoly pricing. Chaos Solitons & Fractals. 1(6), 573-581 (1991)
[17] Agiza H N, Elsadany A.A.: Chaotic dynamics in nonlinear duopoly game with heterogeneous players. Appl. Math. Comput. 149(3), 843–860 (2004)
[18] Elsadany A A.: Competition analysis of a triopoly game with bounded rationality. Chaos Solitons & Fractals. 45(11), 1343-1348 (2012)
[19] De Paula A S, Savi M A.: Comparative analysis of chaos control methods: A mechanical system case study. International Journal of Non-Linear Mechanics. 46(8), 1076-1089 (2011)
[20] Pyragas K.: Continuous control of chaos by self-controlling feedback. Physics letters A. 170(6), 421-428 (1992)

Statements and Declarations

Funding

This work is supported by the Fundamental Research Funds for the Central Universities (Grant No. NS2019045).

Competing Interests

The authors have no relevant financial or non-financial interests to disclose.

Author Contributions

All authors participated sufficiently in the work to take public responsibility for the appropriateness of the

method, analysis, and simulation. All authors reviewed the final version of the manuscript and approved it for publication.

Data Availability

The data used to support the findings of this study are available from the corresponding author upon request.